Degradation behavior of MK35x stacks with chromium-based interconnects in steam electrolysis operation

Matthias Riegraf[a], Patric Szabo[a], Michael Lang[a], Rémi Costa[a], Stefan Rothe[b], Stefan Megel[b], Mihails Kusnezoff[b]

[a]German Aerospace Centre (DLR), Institute of Engineering Thermodynamics, Pfaffenwaldring 38-40, 70569 Stuttgart, Germany
[b]Fraunhofer Institute of Ceramic Technologies and Systems, Winterbergstr. 28, 01277 Dresden, Germany

Abstract

The currently ongoing scale-up of high-temperature solid oxide electrolysis (SOEL) requires the understanding of the underlying dominant degradation mechanisms to enable continuous progress in increasing stack durability. In the present study, the degradation behavior of MK35x stacks with chromium-based interconnects (CFY) and electrolyte-supported cells (ESC) developed at Fraunhofer IKTS is investigated. For this purpose, the initial electrochemical performance of a 10-layer stack was extensively characterized in various operating conditions in both fuel cell and electrolysis mode by electrochemical impedance spectroscopy (EIS). Degradation was evaluated during galvanostatic steady-state steam electrolysis operation for more than 3000 h in the temperature range of 800-825°C at a current density of -0.6 A cm^{-2}, corresponding to a steam conversion rate of 75%. EIS analysis was used to separate the different loss contributions in the stack and showed that the ohmic resistance increase was the dominating performance degradation phenomenon. The observed low degradation rates were caused by the decrease of the polarization resistance during electrolysis operation.

Introduction

Reliable long-term operation is a key factor for the wide-scale adoption of SOEL, so significant development efforts are devoted to mitigate degradation of cells and stacks. Degradation rates as low as 0.5% per 1000 h are targeted by the Strategic Research & Innovation Agenda from the Clean Hydrogen Joint Undertaking by 2030.

While some in-depth degradation studies are available on cell level (1, 2), detailed investigations of SOEL stacks with operation for more than 1000 h are rare in literature. Moreover, the stack degradation behavior is only rarely spatially resolved to the individual layers by means of EIS (3).

The MK35x stack platform developed by Fraunhofer IKTS is based on electrolyte supported cells (ESC) with CFY interconnects. The stacks were initially developed for SOFC operation and demonstrated excellent degradation rates of 0.7 %/1000 h for more than 20,000 h and are commercially available.

Here, the degradation behavior of MK35x stacks tuned to operation in electrolysis mode is investigated in detail over >3000 h.

Experimental Procedure

A ten-cell stack of the Mk35x design with metallic CFY interconnects developed by IKTS was operated in steam electrolysis (4-8). The stack has a cross flow design with internal fuel gas and open-air manifolds. Figure 1 shows the explosion view of the stack components and their assembly. The CFY interconnects have a size of 13.0 x 15.0 cm^2 and the electrolyte supported cells an active area of 11.0 x 11.5 cm^2 (127 cm^2). The ESCs use 10Sc1CeSZ electrolytes and are based on IKTS-G5 electrodes optimized for electrolysis operation (9). After a quality check of every component and assembly, the stacks were sealed, joined, reduced and pre-tested at IKTS (8). The 10-cell stack test was performed in a test rig at DLR with controlled air and gas preheaters. The 10 repeat units (RUs) were numbered upwards from the bottom. The temperatures at the inlets and outlets of the stack as well as the temperatures at three different positions inside the stack (T_5 in RU 5, T_6 in RU 6, T_{10} in RU 10) were monitored. All gas constituents were supplied by mass flow controllers.

After heating up with 2 K/min, the gas-tightness of the different RUs was checked at an air outlet temperature of 770°C with a fuel gas mixture of 40 % H_2/60% N_2. A total air flow of 20 SLPM was used for all tests. Then, an initial current-voltage (jV) performance characterization was carried out in fuel cell and electrolysis mode. Subsequently, a steam electrolysis durability test was started. The inlet fuel gas composition was 80% H_2O and 20% H_2, and a total fuel gas flow rate of 8.8 SLPM with a current density of -600 mA cm^{-2} was used during the durability test leading to a steam conversion (SC) of 75 %. At the beginning of the durability test the oven temperature was adjusted in order to reach 816°C for the oxygen side outlet temperature, and was afterwards held constant during the following durability test. Before cooling down, an end characterization of the stack's performance was carried out at different rated power.

The stack was characterized by means of EIS at a current density of -0.39 mA cm^{-2} with a total fuel gas flow rate of 5.8 SLPM (steam conversion of 75%). These operating conditions were chosen in order to improve data quality of the spectra. The oven temperature was adjusted for the oxygen side outlet temperature to reach 800°C. EIS was carried out with a 'Zahner IM6' impedance analyzer connected to an electronic load 'EL1000'. A voltage supply was integrated in the current circuit for SOEC measurements. An AC amplitude of 15 mA cm^{-2} with a frequency range of 20 mHz to 20 kHz was applied to the stack. The electrical current probes were connected to the top and bottom plates, while the voltage probes were attached at each repeat unit of the stack enabling EIS measurements at all single repeat units.

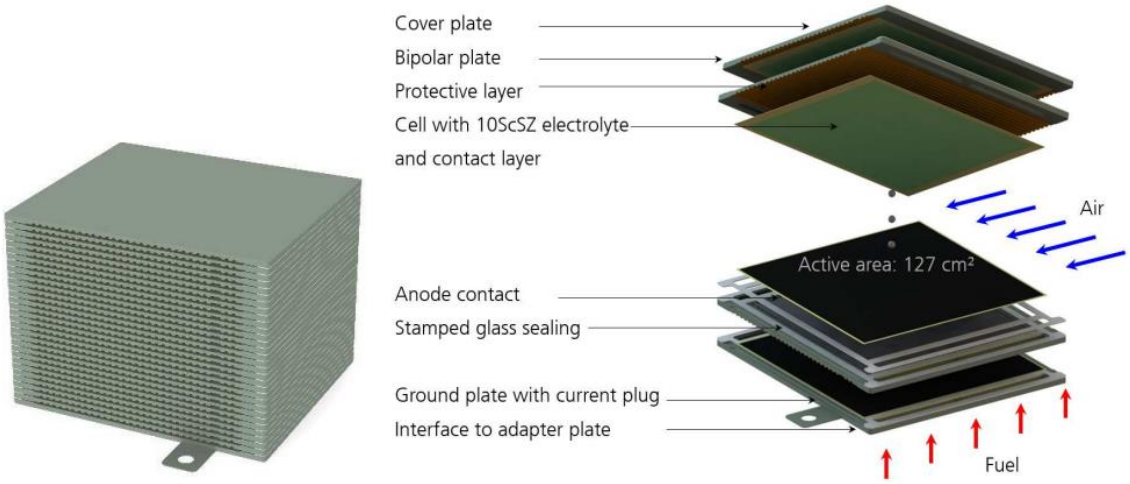

Figure 1. Illustration of a MK35x stack. 30-cell stack (left) and its explosion view (right) (5).

Results and Discussion

Electrochemical characterization in fuel cell operation

Initial characterization of the stack in fuel cell operation was performed during initialization. A diagram comprising the homogeneity of the voltages of the single RUs at OCV and at 0.28 A cm^{-2}, as well as their calculated ASR values is shown in Figure 2. Additionally, the reference values obtained during the initialization procedure at IKTS are depicted for comparison.

All OCV values except RU 1 were above 1.2 V confirming a generally good gas-tightness of the utilized setup and the stack. The OCV of the first RU was slightly below 1.2 V indicating a small leakage at the sealing of the base plate to the external manifold.

The voltage values of RUs at 0.28 A cm^{-2} ranged between 0.778 V and 0.810 V, and their distribution over the stack height was in good agreement with the values obtained during the pre-test at IKTS. The difference between the voltage values for the different RUs measured at DLR and IKTS was in the range of 8-25 mV, and was most likely due to a lower temperature of the air preheater at DLR. ASR values were derived from the impedance spectra depicted in Figure 3 and were between 0.918 Ω cm^2 and 1.157 Ω cm^2. The distribution of both the ASR and the voltage over the height of the stack showed good agreement with a lower performance at the bottom and top RUs and slightly higher performance of the RUs in the middle of the stack. At this operating point, temperatures of 845°C in RU 6 and 837°C in RU 10 were measured showing a non-uniform temperature distribution inside the stack. This is a well-known behavior for stacks in SOFC operation caused by the so-called “edge effect” (10). During operation, the heat losses from the outer RUs to the top or bottom plate of the stack are higher compared to the RUs in the middle which have lower heat transfer to their adjacent RUs. Thus, higher temperatures occur in the middle cells, leading to lower resistances.

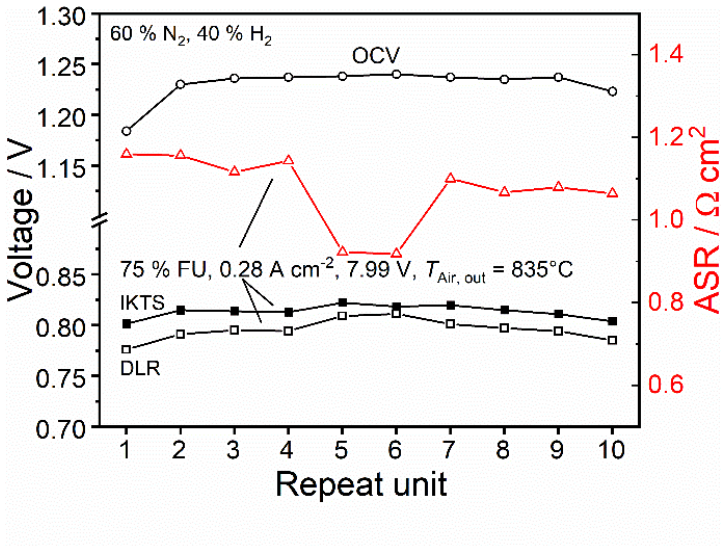

Figure 2. Diagram depicting voltage and ASR homogeneity of the RUs inside the stack in SOFC operation with a fuel gas consisting of 60 % N_2, 40 % H_2. Voltage values are shown at OCV and at 0.28 A cm^{-2}. Reference values obtained at IKTS are inserted for comparison.

Impedance spectra of all RUs measured at 0.28 A cm^{-2} are shown in Figure 3. At the high-frequency range of the spectra different inductance phenomena (high frequency artefacts) occurred that hinder the quantitative comparison of the ohmic resistance values of the RUs. However, as a general trend it can be observed that the ohmic resistances of the outer RUs are increased compared to the RUs in the middle of the stack reflecting the above-mentioned temperature gradient in the stack. However, the main reason for the significantly improved performance of RU 5 and RU 6 in Figure 2 is their low polarization resistance at frequencies ~0.5 Hz whereas the imaginary parts of all spectra show a similar behavior at higher frequencies. For further analysis of the loss contributions in the impedance spectra, a DRT analysis of selected RUs was performed and the results are shown in Figure 3c. At least four peaks could be observed at frequencies of ~5 10^3 Hz, ~10^2 Hz, ~10 Hz and ~0.5 Hz. In previous work, the Ni/CGO fuel gas surface contribution of a G3 cell from IKTS was reported at frequencies of ~5 Hz in SOFC operation (11). Thus, it is possible that the DRT peak identified at 10 Hz in the present study corresponds to this process. The peaks identified at higher frequencies could be related to the Ni/CGO bulk process, an oxygen electrode and corresponding interface processes (12). The gas conversion impedance is often reported of low frequencies of ~0.5 Hz (3), and hence, its variation between the different RUs which is correlated with gas flow distribution between the planes in the stack is the most likely explanation for the differences in performance. However, a more detailed parameter variation is required for an attribution of the loss contributions in the impedance spectra to distinct physico-chemical processes.

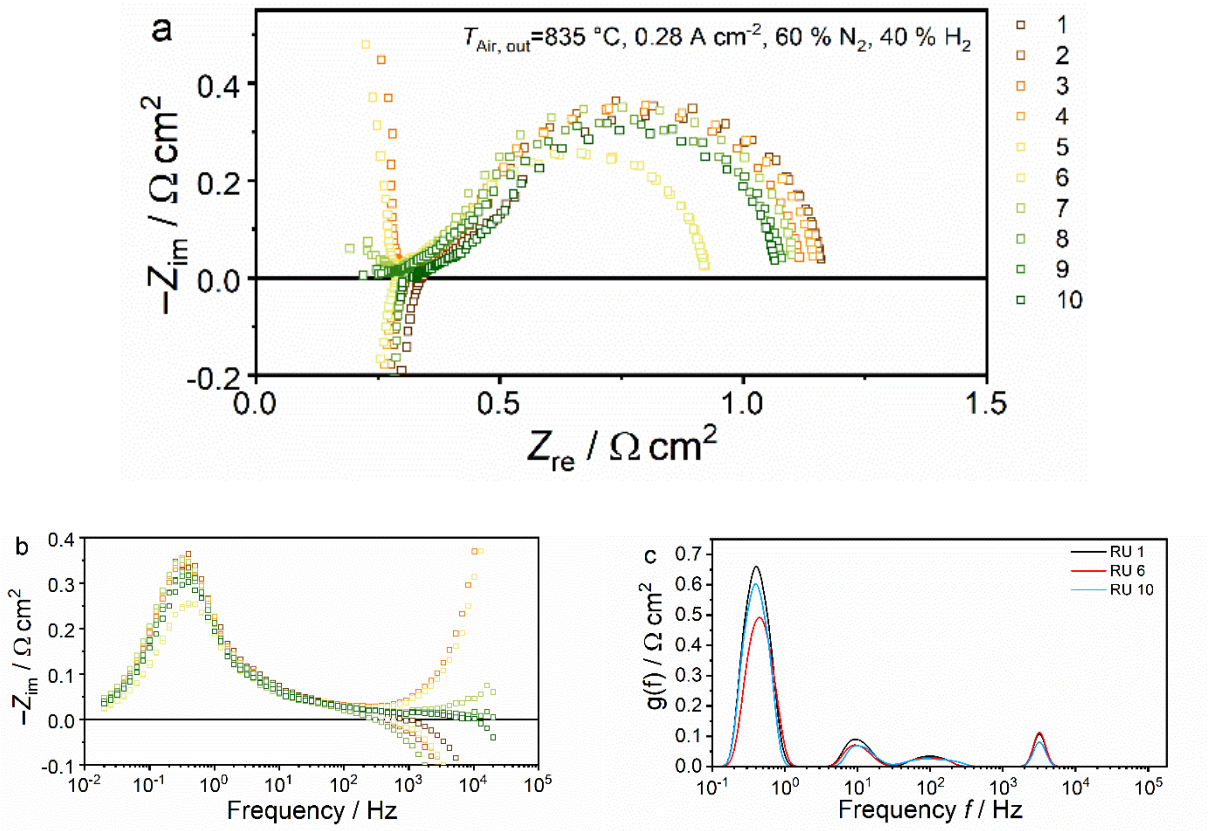

Figure 3. (a) Nyquist plot, (b) imaginary impedance plot and (c) DRT analysis of EIS measurements in SOFC operation with a fuel gas consisting of 60 % N_2, 40 % H_2 at 0.28 A cm^{-2}.

Electrochemical characterization in electrolysis operation

After initial characterization in SOFC, the stack was electrochemically characterized by means of EIS in SOEC operation as well. Figure 4 shows a diagram of the voltage homogeneity of the different RUs at two operating points with fuel gas inlet mixtures of 80 % H_2O + 20 % H_2 and a steam conversion of 75%. Figure 4a shows the homogeneity diagram before the subsequent durability test of -0.6 A cm^{-2} with an oxygen side outlet temperature of 816°C and Figure 4b the diagram at a current density of -0.39 A cm^{-2} and an oxygen side outlet temperature of 800°C. The OCV values of the RUs in both cases are very homogeneous with a maximum deviation of 5 mV. The voltage values at -0.6 A cm^{-2} and -0.39 A cm^{-2} are within a range of 118 mV and 98 mV, respectively. The homogeneity diagram in both cases shows a similar behavior over the height of the stack with an edge effect displaying the highest voltage values close to the top and bottom plates. Temperature measurements within the stack showed a maximum difference of 3 K and 6 K between RU 6 and RU 10 at -0.39 A cm^{-2} and -0.6 A cm^{-2}, respectively, which is considerably lower than the 8 K observed in fuel cell operation at lower overpotentials. This demonstrates that thermal gradients are significantly less pronounced in SOEC operation close to the thermoneutral voltage due to the compensation of the endothermal steam splitting reaction by the Joule heating within the stack.

Moreover, in contrast to the initial characterization in SOFC operation, RU 7 shows the lowest voltage. For further analysis, impedance spectra of selected RUs at -0.39 A cm^{-2} are displayed in Figure 5. RU7 shows the lowest ohmic resistance among all cells, which is most

likely the reason for its low operating voltage. Considerable scattering of the impedance data in the low-frequency region impeded an exact determination of the polarization resistance. However, compared to the EIS measurements in SOFC operation in Figure 3, only small deviations were observed in the polarization resistance indicating a homogeneous feed gas distribution within the stack in SOEC mode. This difference in behavior is caused by a far lower contribution of the gas conversion impedance to the total ASR at higher steam content in the gas mixture (it is highest for a dry H_2/N_2 mixture).

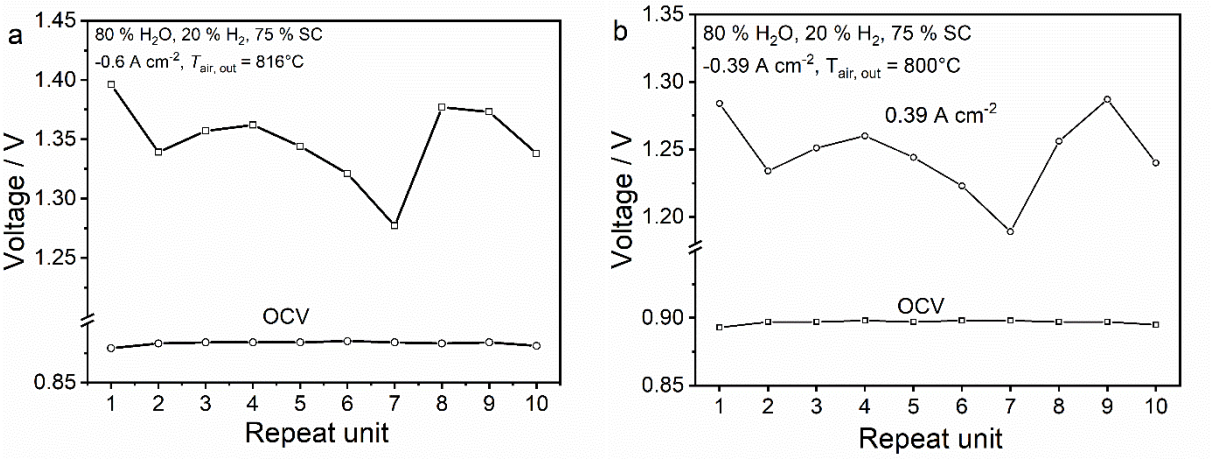

Figure 4. Homogeneity diagram depicting voltage of the RUs inside the stack in SOEC operation with a fuel gas consisting of 80 % H_2O + 20 % H_2. Voltage values are shown at OCV and at (a) -0.6 A cm^{-2} and (b) -0.39 A cm^{-2}.

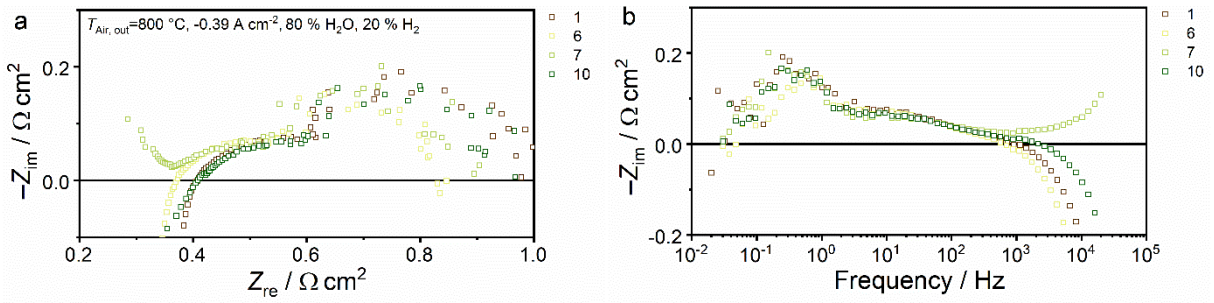

Figure 5. (a) Nyquist plot, (b) imaginary impedance plot of selected EIS measurements in SOEC operation with a fuel gas consisting of 80 % H_2O, 20 % H_2 at -0.39 A cm^{-2}.

Long-term stability in electrolysis operation

After initial stack characterization, a SOEC durability test was performed at -0.6 A cm^{-2} and with an initial oxygen side outlet temperature of 816°C. The entire long-term behaviour of the stack is depicted in Figure 6. The degradation test stretched over an overall time of ~5000 h during which the stack was operated for 3261 h at the nominal operating conditions. Significant voltage oscillations occurred especially in the first half of the test due to instabilities in the steam supply, but were resolved later by optimized operation of the humidifier. The operating time was subdivided into four periods (see Table 1) between which the test rig had to be cooled

down for technical maintenance. Table 1 summarizes the degradation rates during all four periods and for the entire durability test.

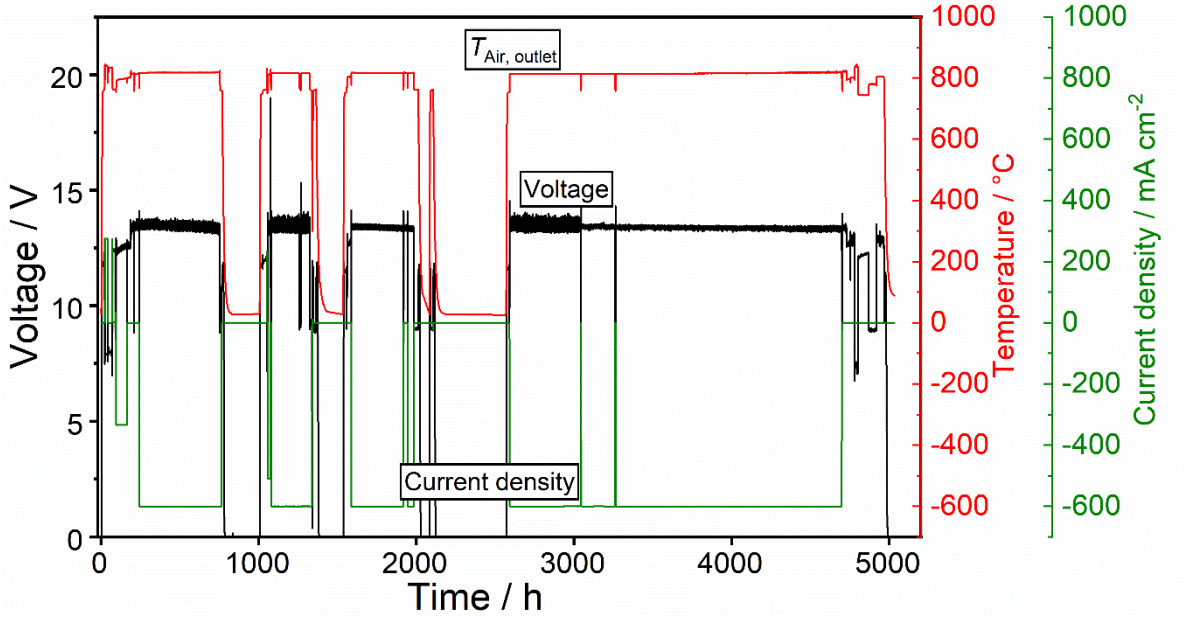

Figure 6. Long-term test of the stack at -0.6 A cm^{-2} (75 % SC) with 80 % H_2O + 20 % H_2 and air.

Table I shows an increase of the stack voltage in the operating phases 1, 3 and 4 leading to negative degradation rates, that is, an improvement of the performances in these time periods. During phase 2 a small degradation of 74 mV was observed. Over the course of the whole 3261 h at the nominal operating point including the three thermal cycles, also a negative degradation rate of -45 mV/1000 h was observed which corresponds to an improvement of -0.33 %/1000 h and demonstrates the outstanding stability of the MK35x stack in SOEC operation.

TABLE I. Overview of the voltage evolution and degradation during the four periods of operation at the nominal operating point -600 mA cm^{-2} (75 % SC) with 80 % H_2O, 20 % H_2 and air.

	Phase 1	**Phase 2**	**Phase 3**	**Phase 4**	**Total**
Beginning	244	1084	1595	2599	244
End	751	1321	1983	4728	4728
Length [h]	507	237	388	2129	3261
Initial voltage [V]	13.465	13.381	13.367	13.462	13.465
End voltage [V]	13.266	13.455	13.277	13.317	13.317
Absolute voltage change [mV]	-199	64	-90	-145	-148
Degradation rate [mV/1000 h]	-392	270	-232	-68	-45
Relative degradation [%]	-1.48	0.48	-0.67	-1.08	-1.1
Relative degradation rate [%/1000 h]	-2.92	2.02	-1.74	-0.51	-0.33

For an in-depth understanding of this activation behavior, representative electrochemical impedance spectra of RU 6 over time are depicted in Figure 7. The spectra show an increase of the ohmic resistance over time which is commonly reported as the dominant degradation process for ESC. Most likely it is predominantly caused by a gradual decrease of the ionic conductivity of the doped zirconia electrolyte (13-15). However, simultaneously the polarization resistance showed a pronounced decrease over time, in particular in the frequency

region of ~10 Hz tentatively ascribed to the Ni/CGO surface process above. However, the frequency range could also be related to the oxygen electrode which was optimized for operation in electrolysis. The underlying reason for this activation effect remains unclear so far. At the operating conditions displayed in Figure 7, the decrease of the polarization resistance could not fully compensate for the increase of the ohmic resistance, leading to a degradation of the total ASR over time. This ASR increase also resulted in an increase of the stack voltage from 12.277 V after 200 h to 12.789 V after 1570 h and 12.846 V after 4942 h during the consecutive recording of the EIS spectra at -0.39 A cm^{-2}. This increase corresponds to an overall degradation of 569 mV and 4.6 %, which amounts to a degradation rate of 1.4 % /1000 h when normalized to the nominal operating period of 3261 h. Thus, the stack showed a different behavior depending on the considered operating conditions. Most likely the different current densities and operating temperatures led to different values of polarization resistance decrease and ohmic resistance increase. This led to an observed negative degradation rate over the course of the experiment during the degradation test in Figure 6, whereas the impedance spectra in Figure 7 showed an actual increase in ASR over time.

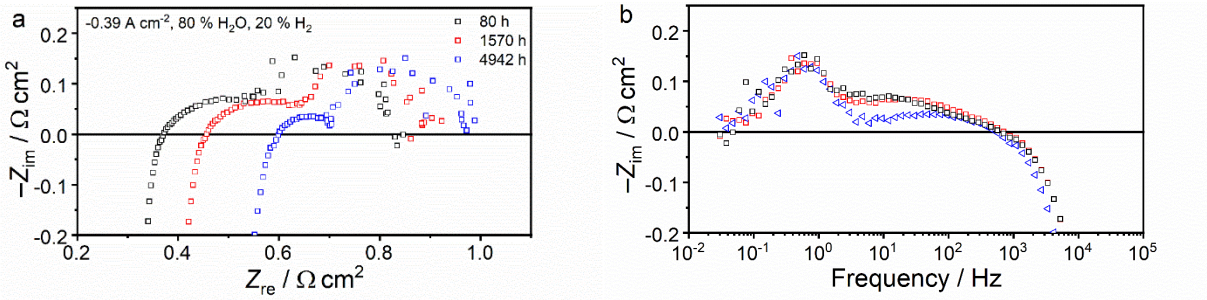

Figure 7. (a) Nyquist plot, (b) imaginary impedance plot of representative EIS spectra of RU 6 in SOEC operation with a fuel gas consisting of 80 % H_2O + 20 % H_2 at -0.39 A cm^{-2}.

Summary and Conclusions

In the present study, the degradation behavior of MK35x stacks developed at Fraunhofer IKTS was investigated. An initial electrochemical characterization of the individual RUs of the 10-layer stack by means of EIS revealed in SOFC and SOEC operation different performance gradients over the height of the stack demonstrating the different temperature and feed gas distributions. A steady-state degradation test in steam electrolysis over >3000 h at a current density of -0.6 A cm^{-2} showed a negative overall degradation rate (improvement) of -0.33 %/1000 h demonstrating the stability of the stack in steam electrolysis. EIS measurements over time were demonstrated to be a useful in unraveling the stack's degradation behavior and revealed increase of the ohmic resistances and decrease of the polarization resistance. The underlying mechanism will be further investigated by a post-mortem analysis in future experiments.

Acknowledgements

The German Ministry of Education and Research (BMBF) is acknowledged for funding in the framework of the “SOC-Degradation 2.0” project under grant number 03SF0621B.

References

1. M. P. Hoerlein, M. Riegraf, R. Costa, G. Schiller, and K. A. Friedrich, *Electrochim. Acta*, **276** 162-175 (2018).
2. J. Schefold, A. Brisse, and H. Poepke, *Int. J. Hydrogen Energy*, **42** (19), 13415-13426 (2017).
3. M. Lang, S. Raab, M. S. Lemcke, C. Bohn, and M. Pysik, *Fuel Cells*, **20** (6), 690-700 (2020).
4. M. Kusnezoff, M. Jahn, S. Megel, E. Reichelt, N. Trofimenko, G. Herz, W. Beckert, J. Schilm, A. Rost, and J. Schoene, *ECS Transactions*, **103** (1), 307 (2021).
5. M. Kusnezoff, S. Megel, C. Rix, P. Adam, E. Reichelt, G. Herz, M. Jahn, N. Trofimenko, and A. Michaelis, *ECS Transactions*, **91** (1), 2579 (2019).
6. S. Megel, C. Dosch, S. Rothe, C. Folgner, N. Trofimenko, A. Rost, M. Kusnezoff, E. Reichelt, M. Jahn, A. Michaelis, C. Bienert, and M. Brandner, *ECS Transactions*, **78** (1), 3089 (2017).
7. S. Megel, C. Dosch, S. Rothe, M. Kusnezoff, N. Trofimenko, V. Sauchuk, A. Michaelis, C. Bienert, M. Brandner, and A. Venskutonis, *ECS Transactions*, **57** (1), 89 (2013).
8. S. Megel, M. Kusnezoff, N. Trofimenko, V. Sauchuk, A. Michaelis, A. Venskutonis, K. Rissbacher, W. Kraussler, M. Brandner, and C. Bienert, *ECS Transactions*, **35** (1), 269 (2011).
9. N. Trofimenko, M. Kusnezoff, S. Mosch, and A. Michaelis, *ECS Transactions*, **91** (1), 263 (2019).
10. M. Lang, C. Auer, G. Braniek, F. Wenz, and F. Hauler, *ECS Transactions*, **68** (1), 2441 (2015).
11. M. Riegraf, M. P. Hoerlein, R. Costa, G. Schiller, and K. A. Friedrich, *ACS Catalysis*, **7** (11), 7760-7771 (2017).
12. M. Riegraf, F. Han, N. Sata, and R. Costa, *ACS Applied Materials & Interfaces*, **13** (31), 37239−37251 (2021).
13. J. Kondoh, T. Kawashima, S. Kikuchi, Y. Tomii, and Y. Ito, *J. Electrochem. Soc.*, **145** (5), 1527-1536 (1998).
14. A. Müller, A. Weber, and E. Ivers-Tiffée, *in* "Proceedings of the sixth European Solid Oxide Fuel Cell Forum", Vol. 28, p. 1231-1238, 2004.
15. F. T. Ciacchi and S. P. S. Badwal, *J. Eur. Ceram. Soc.*, **7** (3), 197-206 (1991).